European Journal of Orthodontics 31 (2009) 12–20
doi:10.1093/ejo/cjn066
Advance Access publication 15 December 2008

Numerical/experimental analysis of the stress field around miniscrews for orthodontic anchorage

A. Gracco*, A. Cirignaco*, M. Cozzani*, A. Boccaccio**, C. Pappalettere** and G. Vitale**

*Department of Orthodontics, University of Ferrara and **Department of Mechanical and Management Engineering, Politecnico di Bari, Italy

SUMMARY The aims of this study were to analyse the stress distribution developing around an orthodontic miniscrew (OM) inserted into the maxilla and to determine the stress field changes for different screw lengths and for different levels of osseointegration occurring at the bone/screw interface.

An integrated experimental/numerical approach was adopted. Using the photoelastic technique, the stress field arising in the bone after screw insertion and the application of the initial orthodontic load was assessed. The finite element (FE) method was used to determine the stress acting in the bony tissue after a given time following screw application, when, for the viscoelastic relaxation effects, the only stress field remaining was that due to the application of the orthodontic load. Different levels of osseointegration were hypothesized.

Photoelastic analyses showed that stress distribution does not change significantly for moderate initial orthodontic loads. From the FE simulations, it was found that critical conditions occur for screws 14 mm long with an orthodontic load of 2 N. The optimal screw length seems to be 9 mm. For such a dimension, small stress values were found as well as low risk of lesion to the anatomical structures.

Introduction

A critical issue related to skeletal anchorage realized with orthodontic miniscrews (OMs) is the mechanical behaviour of miniscrews inserted into the upper and lower jaws. The bone remodelling processes occurring at the bone/screw interface and the screw mobilization mechanisms are strictly correlated with the structural response of the bony tissue to the OMs and then to the stress/strain field developing within the OMs itself and within the surrounding bone. Although orthodontic loads are not sufficiently heavy to cause miniscrews to fail, the stress produced by the forces applied when the screws are removed may cause critical conditions of incipient failure for the miniscrews, especially in cases of osseointegration. At removal, the stress is concentrated at the neck of the screw. If an Allen wrench is used for insertion and removal, the hole in the centre of the screw will weaken the neck, which may lead to fracture (Dalstra *et al.*, 2004; Melsen, 2005). Miniscrews are self-threading and currently tend to be made with a reduced diameter of 1.3–1.5 mm. However, an excessively small resistant transverse section may lead, especially in the insertion phase, to high stress concentrations, even close to those of failure (Carano and Melsen, 2005; Carano *et al.*, 2005). A study on the load transfer of OMs has been conducted by Dalstra *et al.* (2004). They used the finite element (FE) method to investigate the stress/strain field within the bone surrounding the Aarhus Anchorage® screw. Motoyoshi *et al.* (2005) studied the biomechanical effect of abutment on stability of orthodontic mini-implants. They found remarkable differences between the stress distribution computed for models with and without abutment teeth.

Studies of stress allow optimization of the shape of the screw and of its geometric parameters such as length, diameter, and thread pitch. Furthermore, analysis of the stress arising around miniscrews could be utilized in computational mechano-biological models (Pauwels, 1960; Prendergast *et al.*, 1997; Carter *et al.*, 1998; Gòmez-Benito *et al.*, 2005) in order to study bone remodelling and the tissue differentiation processes occurring in the vicinity of the screw. A comprehensive analysis of the mechanical behaviour of miniscrews and of the bone structural response during the period from insertion to when a given level of osseointegration is achieved at the bone/screw interface has yet to be carried out.

The aim of this research was to analyse the stress distribution which develops around a miniscrew due both to the insertion of the screw in the maxillary bone, producing the stress field ($\sigma_{insertion}$), and to the application of the orthodontic load on the miniscrew head, producing the stress field (σ_{load}). An integrated numerical/experimental approach was adopted in order to investigate how the load transfer at the bone/screw interface changes for screws of different lengths and for different levels of osseointegration.

Materials and methods

Epoxy resin plates (dimensions: 50 × 40 mm) 15 mm thick were constructed to carry out photoelastic analyses.

A preliminary characterization process was undertaken in order to identify the mechanical and photoelastic properties of the resin. The screw holes were made using a 1.2 mm round bur and twist drill at 500 rpm. The amount of screw insertion into the epoxy resin plate was set such that the entire threaded part of the screw was placed within the hole. A square column geared head mill drill allowed for the placement of the holes perpendicular to the top surface of the resin plates. Refrigeration systems were used in order to decrease, as much as possible, overheating of the plates during drilling.

Miniscrew Anchoarge System screws [Micerium, Avegno (GE), Italy] (Carano *et al.*, 2004, 2005) with a diameter of 1.5 mm and lengths of 7, 9, 11, and 14 mm (Table 1) were progressively inserted into the epoxy resin plates. Once inserted, different loads of 0 [i.e. the only stress field acting is ($s_{insertion}$) due to the screw insertion], 0.5, 1.5, and 2 N were applied on the hole of the OMS head. A set of calibrated weights was used to apply the different loads.

Photoelastic analyses were carried out using a circular polariscope, designed and assembled at the Politecnico di Bari, and employing polarized white light. The polariscope comprised two linear polarizers and two quarter-wave plates. Such a set-up allows the generation of circularly polarized light which permits easy differentiation of isoclines (locus of the points in the specimen along which the principal stresses are in the same direction) and isochromatics (locus of the points along which the difference in the first and second principal stress remains the same). The distance between the edges of the first-order fringes (i.e. the red fringes above and below the screw long axis) d_{fof} was measured for each screw and for each load applied. This distance could be considered representative of the extension of the region surrounding the screw where significant stress arises. In general, greater d_{fof} imply wider regions with high stress levels and thus a higher risk of bone failure and screw mobilization.

In the second part of the study, a FE analysis of the bone/miniscrew coupling was conducted.

Four two-dimensional computer-aided design (CAD), models were generated of conical miniscrews with the same dimensions as those analysed with the photoelastic technique (diameter 1.5 mm, lengths 7, 9, 11, 14 mm); the other dimensions were taken from the CAD models provided by the miniscrew manufacturers. The material comprising the miniscrews was assumed to be titanium, homogeneous, linear elastic, with a Young's modulus of E = 110000 MPa and a Poisson's ratio of ν = 0.3 (Dalstra *et al.*, 2004). The bone surrounding the miniscrew was also modelled in the CAD environment. A 1.5 mm thick layer simulated the cortical thickness (E = 13700 MPa, ν = 0.3), Boccaccio *et al.* (2006), while the inferior region was assumed to be occupied by cancellous bone (E = 1300 MPa, ν = 0.3; Boccaccio *et al.* (2006), Figure 1a). The two models, i.e. the CAD model of the screw and that of the bone, were assembled and placed in contact with each other. Constraints preventing displacements and rotations were applied on three edges of the bone model. A concentrated horizontal force of 2 N was applied to the eye of the miniscrew (Figure 1a). The models of the screw and of the bone were discretized into quadrangular FEs with four nodes, one for each vertex (Figure 1b,c). Non-linear FE analyses were run.

Assessments of the stresses were performed using Von Mises equivalent stress defined by the following equation:

$$\sigma_{equivalent\_Von\_Mises} = \frac{\sqrt{2}}{2}\sqrt{(\sigma_1-\sigma_2)^2+(\sigma_2-\sigma_3)^2+(\sigma_1-\sigma_3)^2},$$

where σ_1, σ_2, and σ_3 are the first, second, and third principal stress, respectively.

Table 1 Geometric parameters of the investigated miniscrew.

Length (mm)	Diameter (mm)	Height of the thread (mm)
14	1.5	8
11	1.5	8
9	1.5	6
7*	1.5	4

*Screws with a length of 7 mm are not currently on the market; this length was obtained by shortening a 9 mm screw.

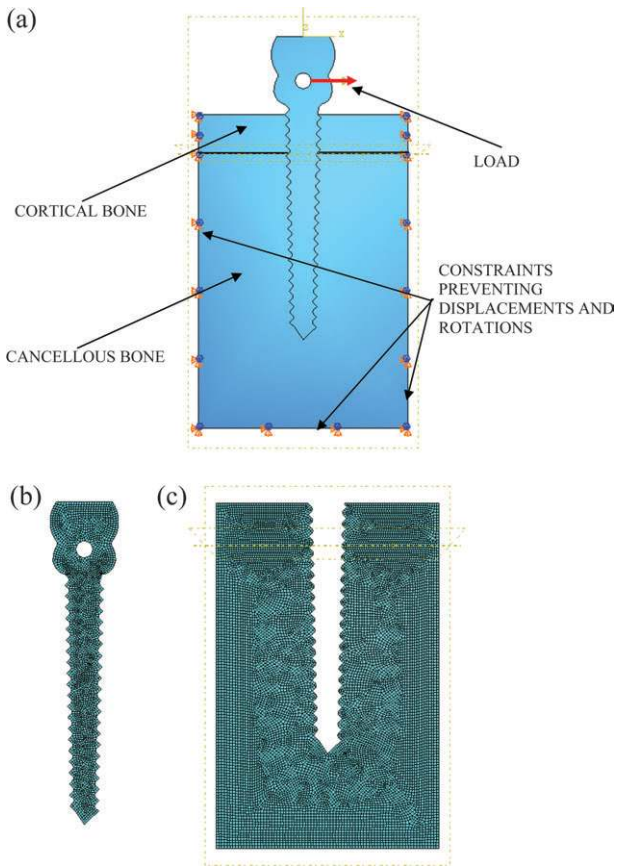

Figure 1 Computer-aided design (CAD) model of the bone and the screw (a), finite element mesh of the screw (b), and of the bone model (c).

No clear information is currently available concerning if and how the osseointegration processes take place at the bone/screw interface. In order to take into account this lack of data, different levels of osseointegration were hypothesized. For each of the four bone-screw models (each corresponding to a different screw length), three FE analyses were run. In the first analysis, 'complete', i.e. along the entire surface of the screw, osseointegration was simulated. In the second, the scenario where no osseointegration occurs at the bone/screw interface was investigated. Finally, an intermediate case (partial osseointegration) was analysed where in some regions of the bone/screw interface osseointegration was hypothesized to have occurred whereas in others no osseointegration had taken place. In the case of complete osseointegration, it was assumed that all the nodes placed at the bone/screw interface and belonging to the screw were 'tied' with their counterparts having the same coordinates, placed at the same interface and belonging to the bone model. Using the tie constraint, stress fields different from zero were computed both when two generic interacting bodies approached one another (compressive stress) (Figure 2c) or when two bodies moved away one from the other (tensile stress) (Figure 2d). In order to simulate no osseointegration, the contact–interaction algorithm was set along the whole bone/screw interface. Such an algorithm simulated the force transfer occurring when two bodies were placed in contact and one is pushed against the other. Stress fields equal to zero were computed using this algorithm if the interacting bodies moved away one from the other (Figure 2b) while stress fields different from zero were computed where the two bodies approached one another (Figure 2a). For partial osseointegration, it was hypothesized that the tie constraint acted on nodes randomly distributed along the bone/screw interface and occupying 50 per cent of its extension. For the remaining nodes, the contact–interaction algorithm was set. Such an assumption was made based on the results of Melsen and Lang (2001) who in monkey models, conducted a study on the biological reactions of the alveolar bone to orthodontic loading of oral implants. Their histological analyses showed that the portion of surface where osseointegration takes place was about half of the entire interface and was not influenced by loading.

An *ad hoc* Fortran routine was developed, a schematic of which is shown in Figure 3. The routine selects firstly the nodes (N_b) localized at the bone/screw interface and belonging to the bone model. Therefore, the algorithm chooses at random, and following a Gaussian distribution, 50 per cent of the aforementioned nodes and records them into the vector (N_{bs}). At this point, the routine selects [and records them into (N_{ss})] the nodes localized at the bone/screw interface, belonging to the screw model and with the same coordinates of those recorded into N_{bs}. The tie constraint is then set for each couple of nodes, of which one belongs to N_{bs} and the other to N_{ss}. The same procedure was adopted for the other nodes occupying the remaining 50 per cent of the interface. However, in this case, the contact–interaction algorithm was set for each couple of nodes.

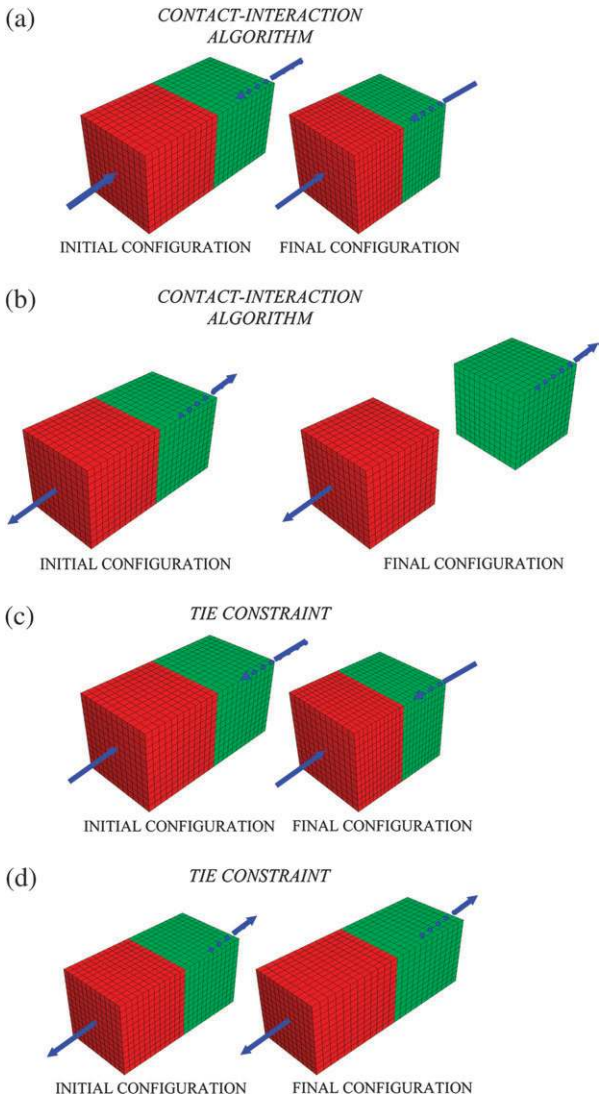

Figure 2 The interaction between two bodies can be simulated either with the 'contact–interaction' algorithm (a–b) and with the 'tie' constraint (c–d). With the contact–interaction algorithm, stress fields equal to zero are computed if the two bodies are moved away from each other (b) while stress fields different from zero are computed where the two bodies approach each another (a). Using the tie constraint, stress fields different from zero are computed both when the two bodies approach each another (compressive stress) (c) or when the two bodies move away one from each other (tensile stress) (d).

It should be noted that the integrated use of the photoelastic technique and of the FE method provides information of the stress around an OMs at different time points. The photoelastic analyses were used to investigate the stress induced by the concomitant insertion of the screw within the bone and the application of the horizontal load (0, 0.5, 1.5, and 2 N) on the screw. In other words, the photoelastic technique served to estimate the stress field given by the sum of the fields ($\sigma_{insertion}$ plus σ_{load}). Such a stress state acts within the bone in the time immediately subsequent to

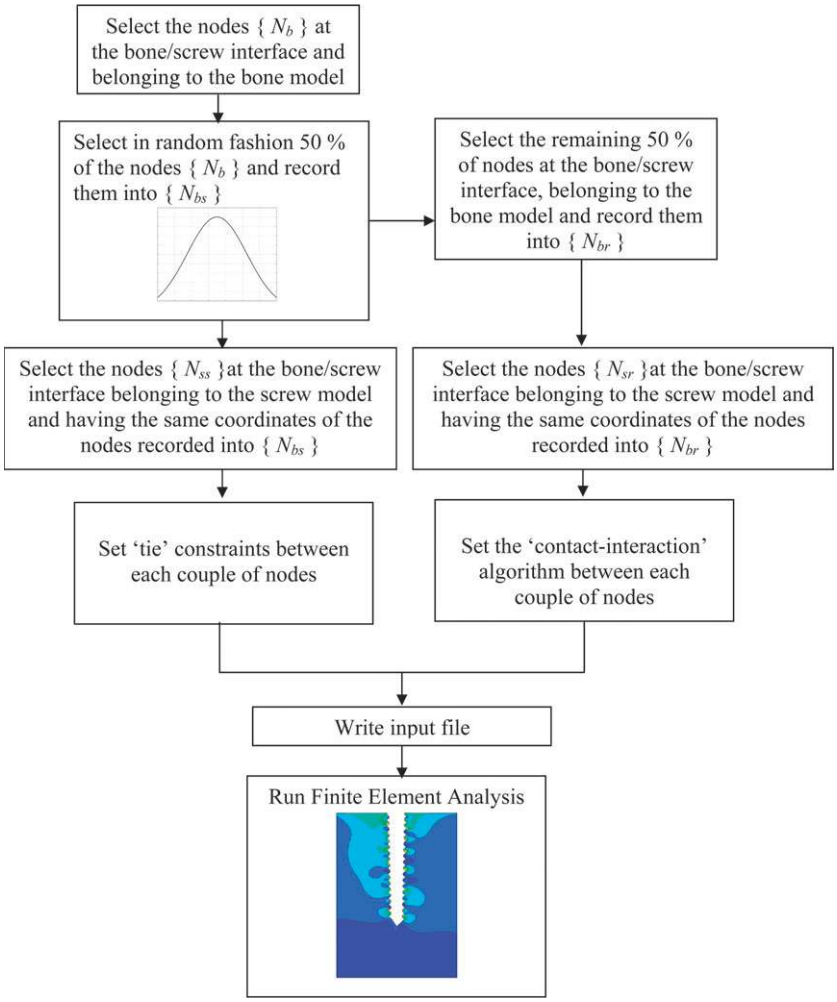

Figure 3 Schematic of the Fortran routine used to simulate partial osseointegration at the bone/screw interface.

miniscrew insertion and the application of the orthodontic load. Conversely, FE analyses neglect the effect of insertion (i.e. $\sigma_{insertion}$). In fact, the bone CAD model reproduced, at the bone/screw interface, exactly the negative of the screw profile. Therefore, the FE model takes into account only the σ_{load} produced by the application of the orthodontic load on the screw head. Such stress could be hypothesized to act on the bone after a given time following screw application, when the viscoelastic phenomena produce a relaxation of the initial stress ($\sigma_{insertion}$) induced by the insertion of the OMS, hence leaving only the effect due to the orthodontic load (σ_{load}). This last effect persists over time as the orthodontic load is consistantly acts on the screw.

Concerning the orthodontic load applied on the miniscrews after a given time following insertion, Motoyoshi *et al.* (2005) and Kuroda *et al.* (2007) reported values not exceeding 2 N. Conversely, for the initial load applied after insertion, different theories are followed. Dalstra *et al.* (2004) calculated the strain developed in various cortical thicknesses and densities of trabecular bone when a load of 0.5 N was placed perpendicular to the long axis of a 2 mm diameter mini-implant. They found that with thin cortical bone and low-density trabecular bone, the strain values may exceed the level of microfractures and thus lead to screw loosening. Miyawaki *et al.* (2003) studied the factors associated with the stability of titanium screws placed in the posterior region for orthodontic anchorage. They concluded that immediate loading is possible if the applied force is less than 2 N. Therefore, for the FE model, simulating the load transfer in the bone/screw coupling after a given time following insertion, a load of 2 N was applied whereas in the photoelastic analyses, simulating the load transfer in the bone/screw coupling immediately after screw insertion, four loads of 0, 0.5, 1.5, and 2 N were applied on the screw head, to investigate the effects of initial loading.

Results

From the photoelastic analyses, increasing orthodontic loads lead to greater distances between the first-order fringes

d_{fof} (Figure 4). The minimum value $d_{fof\text{-}min}$ of this distance was found for the 9 and 14 mm screws in the absence of orthodontic loads. Figure 5 shows the percentage increase (computed with respect to $d_{fof\text{-}min}$) of d_{fof} for the different orthodontic loads and screw lengths investigated. The distance between the first-order fringes increased significantly when loads greater than 1.5 N were applied. Furthermore, for loads of 1.5 and 2 N, the distance d_{fof} appeared remarkably sensitive to screw length.

Numerical analyses showed that high values of Von Mises stress arose within the screw and principally at the neck (Figure 6a). However, these values were significantly smaller than the yield strength (σ_y = 880 MPa) (http://www.matweb.com) of titanium of which the miniscrews were made. High stress values were also found within the cortical bone (Figure 6b). Remarkable stress concentrations were computed on the right side, with respect to the longitudinal axis of the screw, in the case of no osseointegration (Figure 6b). High concentrations were predicted on both sides for partial or complete osseointegration. Specifically, in the latter case, a rather symmetric Von Mises stress distribution was predicted. For the cancellous bone, the patterns of stress also appeared to be very sensitive to the level of osseointegration (Figure 7). For partial osseointegration, high Von Mises stress values were predicted in regions randomly distributed along the bone/screw interface, whereas in the case of complete osseointegration, the Von Mises stress pattern appeared to be symmetric with respect to the screw long axis. Without osseointegration, high stress values were computed on the left side (Figure 7) and the side where high stress values arose within the cortical thickness was opposite to that where high stress values were computed within the cancellous bone.

The numerical model predicted decreasing values for the maximum Von Mises stress both in the cortical and cancellous bone, for increasing levels of osseointegration (Figure 8). However, critical values were found for screws with a length of 14 mm without osseointegrated. For a given level of osseointegration, the lowest Von Mises stress values were calculated for the 11 mm screw. However, shorter screws (9 mm) induced maximum Von Mises stress values significantly smaller than the yield strength of bony tissue.

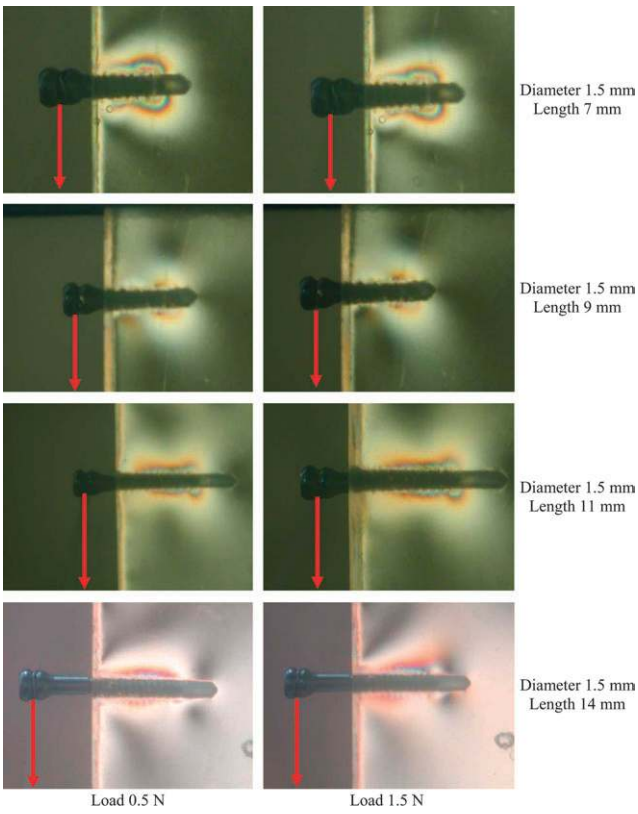

Figure 4 Patterns of photoelastic fringes (isochromatics) observed in the epoxy resin plates under orthodontic loads of 0.5 and 1.5 N.

Discussion

In the present study, a comprehensive analysis of stress distribution induced within the maxillary bone from miniscrews for skeletal anchorage was carried out. The present study has some limitations. Firstly, homogeneous and isotropic epoxy resin plates were used in the photoelastic analyses. In reality the bone, of which a simplified model is represented by the epoxy resin plates, is neither homogeneous nor isotropic. However, it is reasonable to assume that the photoelastic fringe patterns observed with this simplified model provide, with sufficient approximation, a good idea of how the stress pattern is distributed within the maxillary bone. FE analyses aimed to assess how the stress field changes for different levels of osseointegration. Simplified hypotheses were followed in order to identify the regions of the bone/screw interface where osseointegration would occur (Figure 3). The hypothesis of a random distribution of the regions (at the bone/screw interface) where osseointegration takes place was based on the histological observations of Melsen and Lang (2001). Those authors analysed the osteogenetic response occurring in the vicinity of orthodontic implants

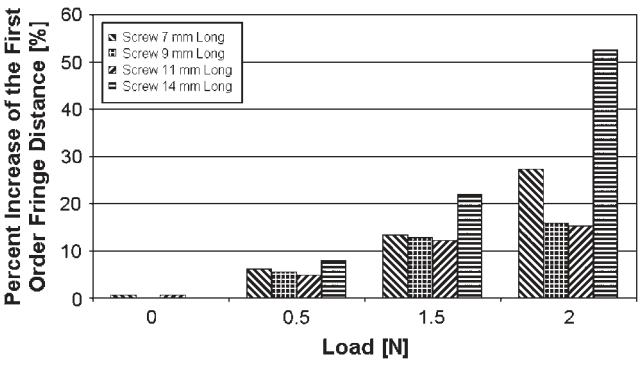

Figure 5 Distance between the first-order fringes for different screw lengths and for different orthodontic loads. The orthodontic load of 0 N corresponds to the situation where the only stress acting within the epoxy resin plates is that due to screw insertion.

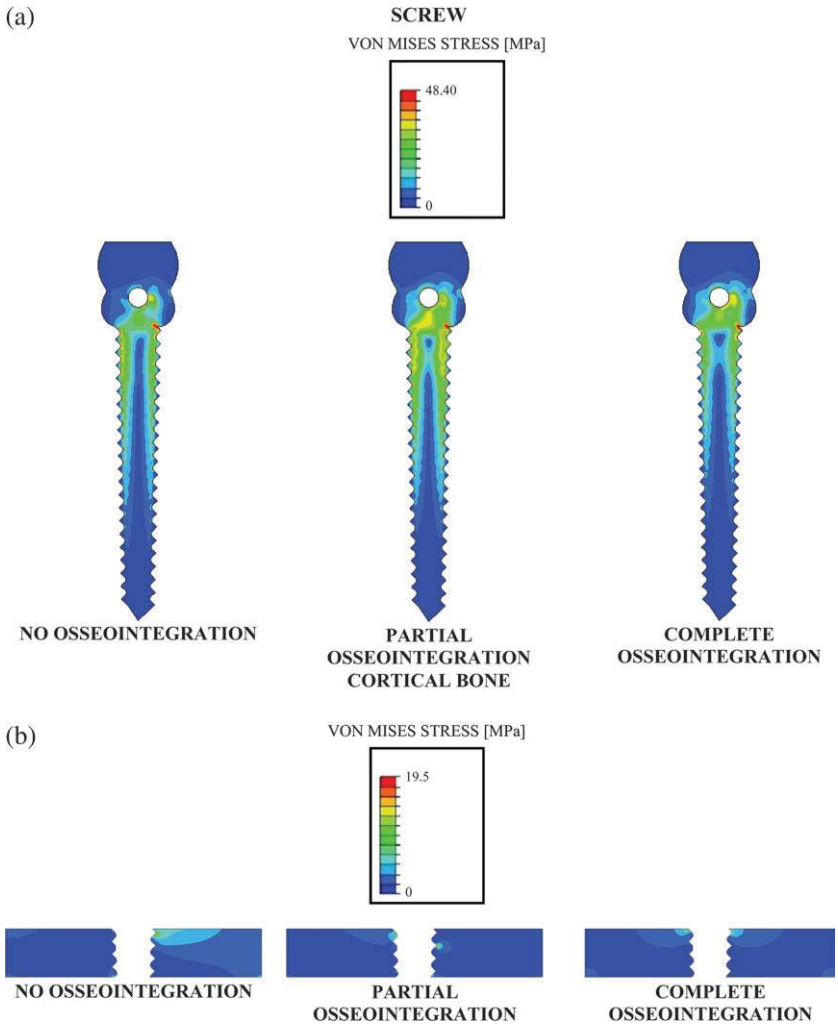

Figure 6 Von Mises Stress distribution in the screw (a) and in the cortical bone (b). The model of a screw 11 mm long is shown.

which, in general, could be different with respect to that occurring for miniscrews. The FE model neglects the stress produced by the insertion of the screw and takes into account only that produced by the horizontal load. Hsieh *et al.* (1999) claimed that stress investigated by FE analyses could be considered to act on the bony tissue at a given time after screw insertion when the viscoelastic phenomena produced a relaxation of the stress field ($\sigma_{insertion}$). Such a hypothesis is supported by the argument that the bony tissue behaves as a viscoelastic material (Les and Spence, 2004; Mano, 2005; Guedes *et al.*, 2006). Furthermore, the same hypothesis of neglecting the stress field ($\sigma_{insertion}$) is implicitly followed by other authors. Motoyoshi *et al.* (2005), when making the diameter of the implant thread and of the bone hole identical, neglected the stress component due to insertion.

Inspite of the aforementioned limitations, the FE predictions in the present investigation are in good agreement with the results of Dalstra *et al.* (2004) who found that when force is applied perpendicular to implants, stress is concentrated in the cortex. This same behaviour was observed in the present study. The Von Mises stress values found in the cortical bone were at least one order of magnitude greater than those computed for the cancellous bone (Figures 6b and 7). High stress concentrations have been found at the neck of the screw by Fongsamootr *et al.* (2006). This is, also, consistent with the results obtained by the proposed numerical model (Figure 6a). The values of Von Mises stresses were of the same order of magnitude as those computed by Motoyoshi *et al.* (2005) in the case of implants without abutments (Figure 8).

Photoelastic analyses showed that the extension of the regions where significant stress concentrations occur does not change significantly if moderate orthodontic loads (not higher than 0.5 N) are applied (Figure 5). Only for higher initial loads (e.g. 1.5 and 2 N) were greater distances d_{fof} measured. It also appears that for higher initial loads, critical conditions can be encountered for 7 and 14 mm long screw. Interestingly, the distance, d_{fof}, appears to be rather insensitive

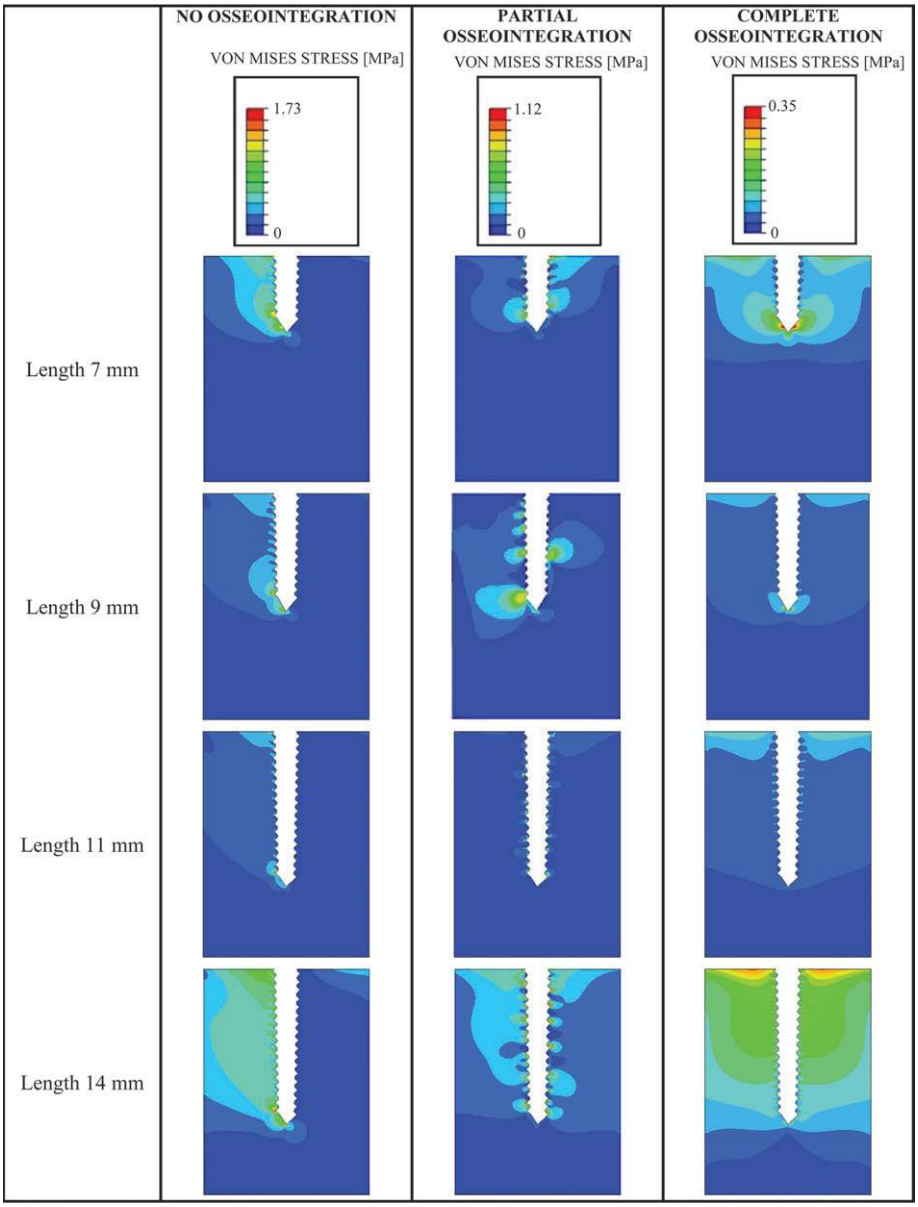

Figure 7 Von Mises Stress distribution in the cancellous tissue for different screw lengths and for different levels of osseointegration.

to screw length for low (less than 1.5 N) initial orthodontic loads while, for higher orthodontic loads (more than 1.5 N), significant differences were measured between the values of d_{fof} corresponding to the different screw lengths.

FE analyses showed that, for a given level of osseointegration, the lowest values of maximum Von Mises stress were computed for screws with a length of 11 mm (Figure 8). Critical conditions were predicted to occur for miniscrews with a length of 14 mm (Figure 8). Specifically, the highest values of maximum Von Mises stress were found both within the cortical (Figure 8a) and cancellous (Figure 8b) bone in the case of no osseointegration. The large increase in stress occurring when the screw length increased from 11 to 14 mm was due to the increase in the bending moment acting on the screw and then on the bone. The portion of screw limited by the head and the point where threading begins (Figure 9) moves the point of application of the load far from the top surface of the bone. Therefore, the load is transferred to the bone with a bending moment given by the product of the load multiplied by the length of this portion. The increase of the maximum Von Mises stress occurring for screws shorter than 11 mm was due to the fact that as the screw length decreased, the surface where bone and screw exchange the interaction forces became smaller resulting in higher stresses. Interestingly, it was found that for the 14 mm screws, the maximum Von Mises stress within the

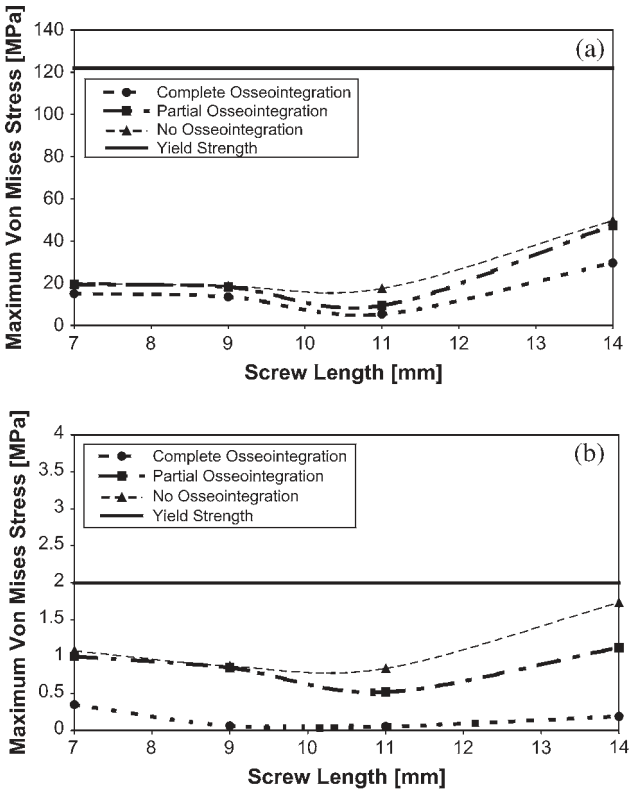

Figure 8 Maximum Von Mises stress computed within the cortical (a) and cancellous (b) bone for miniscrews with different lengths and for different levels of osseointegration.

cancellous bone reached 1.73 MPa, which is very close to the yield strength of 2 MPa of this tissue (Boccaccio *et al.*, 2006). Less significant stress values were found within the cortical bone. A maximum value of 49.65 MPa was calculated which is well below the yield strength limit of 122 MPa (Boccaccio *et al.*, 2006). In general, situations where Von Mises stresses close to the yield strength arise are undesirable and could lead to critical conditions of failure of the bony tissue and then of screw mobilization. Therefore, it is clear that for 14 mm screws, the cancellous bone can undergo failure if loads greater than 2 N are applied.

It was found that for no osseointegration, the side where high stress values arose within the cortical thickness was opposite to the side where high stress values were computed within the cancellous bone. This could be justified by the argument that when the orthodontic load is applied the screw experiences, in addition to a horizontal translation and deformation, a clockwise rigid body rotation about a point localized approximately at the interface between the cortical and cancellous bone. In fact, from Figure 10, showing the trend of the displacement component u_1 along the path AB (on the screw model), it appears that displacements approximately equal to zero were computed at a point at the interface of the cancellous/cortical bone. Smaller rotations were also predicted for partial or complete osseointegration; however, the effects of these rotations in terms of stress were less significant (Figure 7).

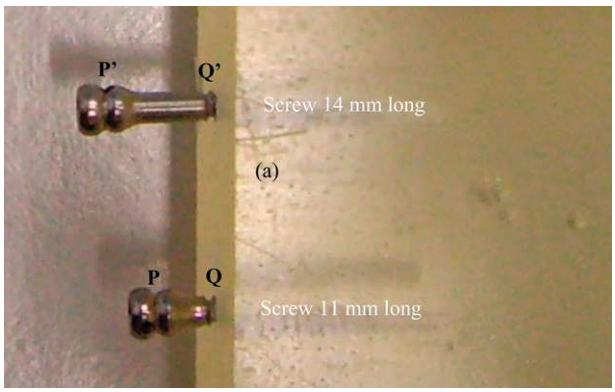

Figure 9 The portion of the screw limited by the point where the load is applied [P (screw 11 mm) and P' (screw 14 mm)] and the point where threading begins [Q (screw 11 mm) and Q' (screw 14 mm)] induces a bending moment in the bone. As the distance P'Q' is greater than the distance PQ, the bending moment arising for the 14 mm screw is greater than that for the 11 mm screw.

In general, it appears that the most favourable situation is that in which partial osseointegration occurs at the bone/screw interface. The Von Mises stresses arising in the bone surrounding a miniscrew partially osseointegrated appeared to be rather uniformly distributed (Figures 6b and 7). In addition, the displacements experienced by the screw were predicted to be very low (about half of those occurring for no osseointegration) (Figure 10). Although lower Von Mises stresses were predicted in the case of total osseointegration, as mentioned, excessive osseointegration occurring at the bone/screw interface can lead to difficulties in miniscrew removal. Thus, partial osseointegration is a good compromise between the necessity of reducing stress and the necessity for easier screw removal.

Conclusions

A comprehensive analysis of the stress distribution induced from miniscrews for orthodontic anchorage within the maxillary bone was carried out. An integrated numerical/experimental approach was adopted in order to determine stress field changes with the use of screws of different lengths and with different levels of osseointegration.

Photoelastic analyses showed that, for moderate initial orthodontic loads, small differences arise between the stress produced by the different screws. High initial loads should be avoided especially when using 14 and 7 mm screws.

FE analyses showed that for 14 mm screws and for loads of 2 N, high Von Mises stress values occur in the bone, which could lead to critical conditions of failure. From this preliminary study, it appears that the optimal screw length is 9 mm. High stress peaks were computed with screws shorter than 9 mm and critical conditions of screw mobilization resulted in high initial orthodontic loads. Screws longer than 9 mm result in a decrease in the stress peaks, but they can lead to a higher risk of lesions of anatomical structures. Partial osseointegration is predicted to be the most preferable level of osseointegration.

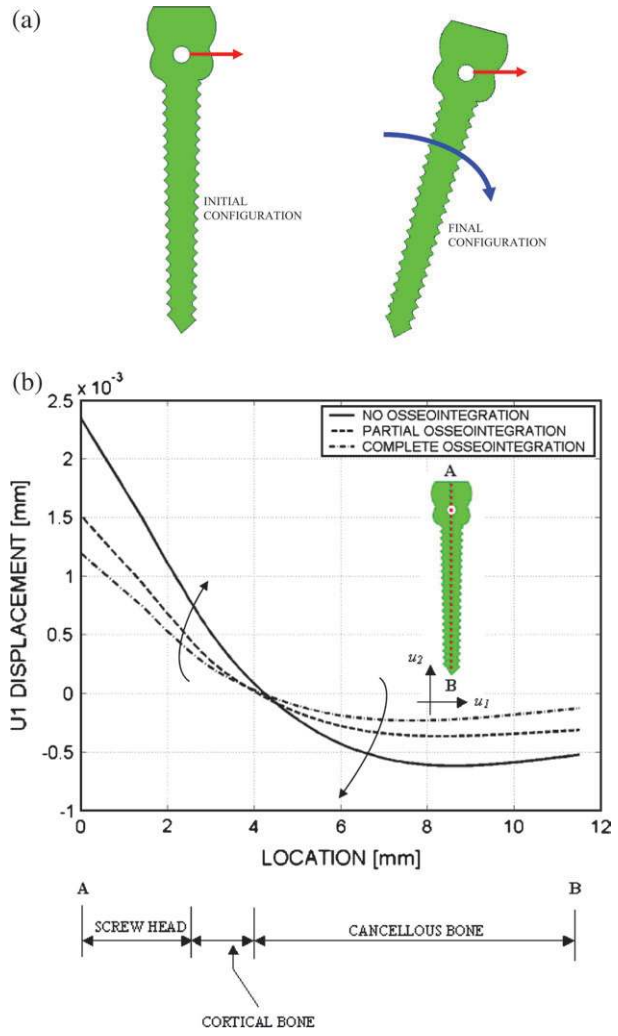

Figure 10 (a) Schematic diagram of the clockwise rigid body rotation experienced by the screw under orthodontic loading and (b) trend of the u_1 displacement component along the path AB for different levels of osseointegration.

A partially osseointegrated miniscrew produces low stress peaks within the bone and the screw is easy to remove.

Address for correspondence

Antonio Gracco
Department of Orthodontics
University of Ferrara
Via Montebello 31
44100 Ferrara
Italy
E-mail: sci@unife.it

References

Boccaccio A, Lamberti L, Pappalettere C, Carano A, Cozzani M 2006 Mechanical behaviour of an osteotomized mandible with distraction orthodontic devices. Journal of Biomechanics 39: 2907–2918

Carano A, Melsen B 2005 Implants in orthodontics. Progress in Orthodontics 6: 62–69

Carano A, Lonardo P, Velo S, Incorvati C 2005 Mechanical properties of three different commercially available miniscrews for skeletal anchorage. Progress in Orthodontics 6: 82–97

Carano A, Velo S, Incorvati C, Poggio P 2004 Clinical applications of the mini-screw-anchorage-system (MAS) in the maxillary alveolar bone. Progress in Orthodontics 5: 212–235

Carter D R, Blenman P R, Beaupré G S 1998 Correlations between mechanical stress history and tissue differentiation in initial fracture healing. Journal of Orthopaedic Research 6: 736–748

Dalstra M, Cattaneo P M, Melsen B 2004 Load transfer of miniscrews for orthodontic anchorage. Orthodontics 1: 53–62

Fongsamootr T, Seehawong N, Buranastidporn B 2006 Three-dimensional finite element analysis of the effect of miniscrew implant length on stress distribution in the miniscrew and cortical bone. Journal of Biomechanics 39: (Supplement 1): S565

Gòmez-Benito M J, Garcìa-Aznar J M, Kuiper J H, Doblaré M 2005 Influence of fracture gap size on the pattern of long bone healing: a computational study. Journal of Theoretical Biology 235: 105–109

Guedes R M, Simões J A, Morais J L 2006 Viscoelastic behaviour and failure of bovine cancellous bone under constant strain rate. Journal of Biomechanics 39: 49–60

Hsieh Y F, Wang T, Turner C H 1999 Viscoelastic response of the rat loading model: implications for studies of strain-adaptive bone formation. Bone 25: 379–382

Kuroda S, Sugawara Y, Deguchi T, Kyung H M, Takano-Yamamoto T 2007 Clinical use of miniscrew implants as orthodontic anchorage: success rates and postoperative discomfort. American Journal of Orthodontics and Dentofacial Orthopedics 131: 9–15

Les C M, Spence C A 2004 Determinants of ovine compact bone viscoelastic properties: effects of architecture, mineralization and remodelling. Bone 35: 729–738

Mano J F 2005 Viscoelastic properties of bone: mechanical spectroscopy studies on a chicken model. Materials Science & Engineering 25: 145–152

Melsen B 2005 Mini-implants: where are we?. Journal of Clinical Orthodontics 34: 539–547

Melsen B, Lang N P 2001 Biological reactions of alveolar bone to orthodontic loading of oral implants. Clinical Oral Implants Research 12: 144–152

Miyawaki S, Koyama I, Inoue M, Mishima K, Sugahara T, Takano-Yamamoto T 2003 Factors associated with the stability of titanium screws placed in the posterior region for orthodontic anchorage. American Journal of Orthodontics and Dentofacial Orthopedics 124: 373–378

Motoyoshi M, Yano S, Tsuruoka T, Shimizu N 2005 Biomechanical effect of abutment on stability of orthodontic mini-implant. Clinical Oral Implants Research 16: 480–485

Pauwels F 1960 Eine neue theorie über den einflu mechanischer reize auf die differenzierung der stützgewebe. Zeitschrift für Orthopädie und ihre Grenzgebiete 121: 478–515

Prendergast P J, Huiskes R, Søballe K 1997 Biophysical stimuli on cells during tissue differentiation at implant interfaces. Journal of Biomechanics 30: 539–548